ELSEVIER

Earth and Planetary Science Letters 171 (1999) 63–81

EPSL

www.elsevier.com/locate/epsl

Fractionation of trace elements by subduction-zone metamorphism — effect of convergent-margin thermal evolution

Gray E. Bebout [a,*], Jeffrey G. Ryan [b], William P. Leeman [c], Ann E. Bebout [d]

[a] *Department of Earth and Environmental Sciences, 31 Williams Drive, Lehigh University, Bethlehem, PA 18015, USA*
[b] *Department of Geology, University of South Florida, Tampa, FL 33620, USA*
[c] *Department of Geology and Geophysics, Rice University, Houston, TX 77251, USA*
[d] *Department of Physical Sciences, Kutztown University, Kutztown, PA 19530, USA*

Received 19 October 1998; revised version received 7 May 1999; accepted 7 May 1999

Abstract

Differential chemical/isotopic alteration during forearc devolatilization can strongly influence the cycling of volatile components, including some trace elements, in subduction zones. The nature and magnitude of this devolatilization effect are likely to be strongly dependent on the thermal structure of individual convergent margins. A recent model for metamorphism of the Catalina Schist, involving progressive underplating (at $\leq$45 km depths) of rock packets metamorphosed along successively lower-T prograde P–T paths in a rapidly cooling, newly initiated subduction zone, affords a unique evaluation of the effects of varying prograde P–T paths on the magnitudes of devolatilization and chemical/isotopic alteration of subducting rocks. In the Catalina Schist, the most extensive devolatilization occurred in metasedimentary rocks which experienced prograde P–T paths encountering the epidote–blueschist facies ($>$350ºC at 9 to 12 kbar) or higher-T conditions; such rocks are depleted in 'fluid-mobile' elements such as N, B, Cs, As, and Sb relative to protoliths. Removal of these elements resulted in changes in B/(Be, Li, La, Zr), Cs/Th, Rb/Cs, As/Ce, Sb/Ce, and $C_{reduced}$/N, and increases in $\delta^{15}N$ and $\delta^{13}C$. The relative susceptibilities of the 'fluid-mobile' elements to loss along increasingly higher-T P–T paths can be categorized. Boron and Cs show the greatest susceptibility to low-T removal by fluids, showing $>$50% depletion in even lawsonite–blueschist-facies metasedimentary rocks which experienced relatively low-T prograde metamorphic paths. In rocks which experienced higher-T paths, As and Sb (likely in sulfides) show the greatest depletions ($>$90%); N, Cs, and B (largely in micas) occur at $\sim$25% of protolith contents in even partially melted amphibolite-facies rocks. Variations in B/Be, Cs/Th, As/Ce, and Sb/Ce among arcs from differing convergent-margin thermal regimes, and conceivably some cross-arc declines in these ratios, are compatible with evidence from the Catalina Schist for varying degrees of element removal as a function of prograde thermal history. In relatively cool subduction zones (e.g., Kuriles, Marianas, Aleutians, southern Alaska) with thermal regimes similar to that which formed the low-grade units of the Catalina Schist (and blueschist-facies rocks in the Franciscan Complex), forearc devolatilization is less profound, B, Cs, As, Sb, and N are more likely to be deeply subducted, and enriched in arc lavas, and significant devolatilization occurs at the blueschist-to-eclogite transition. High-grade units could reflect thermal evolution analogous to that of relatively warm subduction zones (e.g., Cascadia) and back-arcs in which arc lavas are depleted in B, Cs, As, and Sb due to prior removal by forearc devolatilization. The results of this study also imply less efficient recycling of these elements during

* Corresponding author. Tel.: +1-610-758-5831; Fax: +1-610-758-3677; E-mail: geb@chigh.edu

0012-821X/99/$ – see front matter
PII: S0012-821X(99)00135-1

the warmer Archean subduction which resulted in greater slab melting and production of abundant trondhjemite–tonalite magmatic suites.

Keywords: fractionation; trace elements; metamorphism; prograde metamorphism; P–T–t paths; subduction; active margins

1. Introduction

It has become increasingly accepted that large amounts of volatile components in subducted rocks released in forearcs by mechanical expulsion or devolatilization reactions are cycled back through forearc regions to the seafloor (or other shallow reservoirs) or to the mantle, and that this process represents a major variable in the global mantle–ocean mass-balance for some of these components [1–3]. However, the processes by which structurally bound volatile components are released during metamorphism, stored at great depths in accretionary complexes ($\leq$50 km), or subducted to even greater depths have received little attention. Significant attention recently has been paid to the chemical characterization of lithologies being subducted (seafloor sediments and variably altered oceanic crust), in efforts to construct global chemical models and characterize contributions from subducting slabs to arc lavas [4–7].

Studies of modern forearc sediment and pore fluid budgets and arc magmatism provide a rich context into which to place considerations of volatile fluxing at depth in paleoaccretionary wedges. Von Huene and Scholl [8] provided estimates of the magnitudes of forearc sediment accretion, deep sediment subduction, and pore fluid expulsion in their global-perspective analysis of convergent-margin material fluxes. Studies of arc magmatism have pointed to the significance of forearc metamorphic processes in governing the compositions of rocks subducting to regions beneath arc lava source regions [9–12]. Geochemical studies of forearc serpentinite seamounts have also yielded insight regarding the degrees and compositions of forearc fluid fluxing [13–15]. Much research has concentrated on the shallowest manifestations of fluid expulsion from forearcs in trenches on the seafloor and along decollement zones [16]; the shallow fluid budgets are thought to be dominated by the mechanically expelled pore fluid component ([16]; for examples of chemical/isotopic and experimental studies, see [17,18]).

Uplifted tracts of high-P/T metamorphic rocks (e.g., blueschists) preserve information regarding the extents of loss of volatile components during metamorphism along relatively cool $P–T$ paths characteristic of subduction-zone regimes (representing depths of ~15–50 km in ancient (subduction zones; [19]). Recent studies have speculated that the thermal structure of subduction zones influences the efficiency with which volatile components are deeply subducted [20–25]. Cooler subduction-zone thermal regimes (those in which relatively old oceanic lithosphere is being relatively rapidly subducted; [25]) are thought to promote the deep retention of volatiles, perhaps increasing the contributions of volatile components to the deep mantle, including arc lava source regions.

The Catalina Schist (California) records Cretaceous accretion and high-P/T metamorphism, and contains metasedimentary rocks (graywackes and shales) and metamafic rocks (basalts and gabbros) ranging in grade from lawsonite–albite to amphibolite facies (peak conditions of ~275° to 750°C, 5 to 12 kbar; [26,27]; Fig. 1). Forearc metamorphic suites such as the Catalina Schist (and Franciscan Complex) are dominantly composed of the terrigenous sedimentary lithologies (graywacke, shale) thought to dominate the subducted sedimentary inventory (cf. [6,8]). The Franciscan Complex consists of ~80% graywacke, ~10% micro-graywacke and shales, ~10% mafic igneous rocks, and <0.5% chert and associated shale and limestone [28]. The Catalina Schist is similarly dominantly metasedimentary, containing ~70% metagraywacke and metashale, with lesser amounts of metabasalt and metagabbro, metachert, and mélange, and one occurrence of metamorphosed calcareous shale [27]. These sedimentary lithologic proportions are similar to those observed in cores from many carbonate-poor trench environments [6]. Taking into account the deep-ocean pelagic section, and incorporating the massive trench sedimentation (largely sialic) and the additions of sialic material through subduction

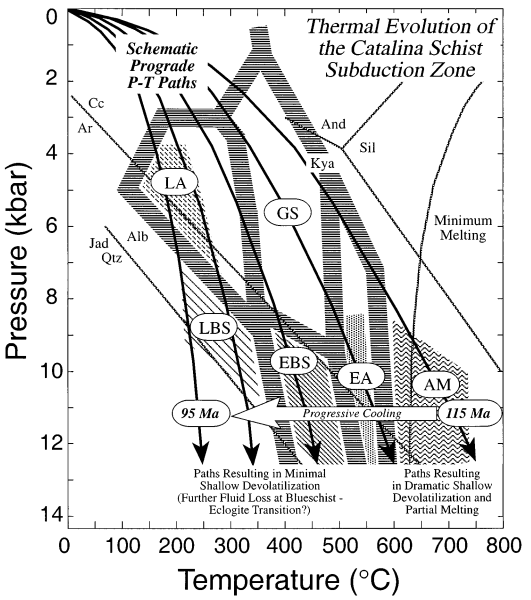

Fig. 1. Pressure–temperature diagram (simplified from [26]) illustrating the varying prograde thermal histories and timing of peak metamorphism and cooling of the tectonometamorphic units of the Catalina Schist. Schematic P–T stability fields of the prograde metamorphism in each of the units (patterned regions); sources of generalized phase equilibria for relevant volcanic and volcaniclastic rocks are given in [26]. The dark lines with arrows represent schematic prograde rock P–T paths in a newly formed subduction zone as a function of time (based in part on the calculations of Peacock [2,56]), with the highest-T path representing the early stages of subduction (labelled *115 Ma*) and other progressively lower-T paths depicting the evolution toward an overall cooler subduction-zone thermal structure (see dark line labelled *95 Ma*). Overall P–T–t loops for each of the units would appear clockwise on this diagram (see fig. 9 in [26]); retrograde paths involving rapid cooling likely resulted in minimal impact of retrogradation on trace element compositions of the prograde metamorphic mineral parageneses. Models of early-stage thermal evolution (see [2]) indicate that significant cooling occurs within a few million years of subduction-zone initiation. Abbreviations for metamorphic facies are as follows: *LA* = lawsonite–albite; *LBS* = lawsonite–blueschist; *EBS* = epidote–blueschist; *EA* = epidote–amphibolite; *GS* = greenschist; *AM* = amphibolite. Mineral abbreviations are: *Jad* = jadeite; *Alb* = albite; *Qtz* = quartz; *And* = andalusite; *Sil* = sillimanite; *Kya* = kyanite; *Cc* = calcite; *Ar* = aragonite.

erosion, von Huene and Scholl [8] estimated that the deeply subducting sediments are ~95% terrigenous, ~3% biogenic carbonate, and ~2% biogenic siliceous rocks. However, the more carbonate-rich pelagic section (~15% biogenic carbonate; [6,29]) may commonly fall below the major decollement in accretionary prisms [8], resulting in preferential deeper subduction of carbonate (in subduction zones with carbonate-rich sediment; [6]) and accounting for its general absence in accretionary complexes.

In the Catalina Schist, the preservation of a coherent set of tectonometamorphic units representing metamorphism at 15–45 km depths in a rapidly cooling subduction zone (see discussion of tectonic model by [26]) allows evaluation of the magnitude of forearc devolatilization as a function of prograde P–T history. The amphibolite-facies rocks are believed to have been accreted to the hanging-wall in the earliest stages of subduction, experiencing the highest-T prograde thermal histories (Fig. 1), whereas lower-grade units were metamorphosed and accreted successively during the progressive cooling of the subduction zone (progressively cooler prograde P–T paths for the lower-grade units). In this paper, we present whole-rock major and trace element data for 42 metasedimentary rocks of the Catalina Schist, integrating these data with previously presented B–Be concentration data and C and N isotope data for the same rocks. We exploit the detailed paleotectonic model for these rocks and present arguments regarding (1) the evidence for trace element mobilization during devolatilization of the Catalina Schist metasedimentary rocks along differing prograde P–T paths, and (2) the extent to which the trace element data for the Catalina Schist can yield insight into the trace element budgets in modern (and ancient) subduction zones with differing thermal evolution. We concentrate on element systems recently used to trace slab + sediment-derived aqueous fluid (and silicate melt) components in arc lavas (B, Be, Li, LILE, U–Th, As and Sb; [5,9–12,14]).

2. Analytical techniques

Whole-rock major and trace element data were acquired for 42 samples of metasedimentary rocks representing the full range in metamorphic grade (Table 1; major element data are reported in the website table; **see EPSL Online Background Dataset** [1]). Boron, Be, and Li concentration data

[1] http://www.elsevier.nl/locate/epsl, mirror site: http://www.elsevier.com/locate/epsl

Table 1
Concentrations of selected trace elements, and ratios among trace element concentrations, in metasedimentary rocks of the Catalina Schist (in ppm unless otherwise specified)

Sample	K_2O [a]	N	Ba	Cs	Rb	Sr	B [a]	Be [a]	Li	La	Ce	U	Th	Zr	As	Sb	B/Be	Cs/Th	Th/U	B/La	B/Li	B/Zr	Rb/Cs	As/Ce	Sb/Ce
Lawsonite–albite																									
7-2-132	1.96	640	459	3.73	70	158	34.5	1.12		12.5	28.7	1.44	4.52	190	4.8	3.01	30.8	0.83	3.14	2.76		0.18	18.8	0.17	0.105
6-3-2a	2.72	695	745	5.60	120	28	69.7	0.97	38.1	11.7	31.1	1.60	4.70	192	5.3		71.9	1.19	2.94	5.96	1.83	0.36	21.4	0.17	
6-3-2f	2.35	410	491	5.10	110	50	102.5	0.86	31.3	15.6	37.1	1.30	5.10	188	4.4		119.2	1.00	3.92	6.57	3.27	0.55	21.6	0.12	
9-1-33	1.26	200	525	1.60	52	59	21.7	0.81	44.8	19.5	44.7	1.10	3.20	127	62.0		26.8	0.50	2.91	1.11	0.48	0.17	32.5	1.39	
6-3-2k′(1)	4.40	900	713	7.30	160	25	181.3	1.26	32.2	16.6	35.8	1.90	6.10	238		2.40	143.9	1.20	3.21	10.92	5.63	0.76	21.9		0.067
6-3-2k′(3)		810	683	7.20	162		106.3	1.00		12.2	27.7	1.90	6.10	115	11.3	2.80	106.3	1.18	3.21	8.71		0.92	22.5	0.41	0.101
6-3-2g	1.54	540	489	3.20	79	282	40.0	1.16	8.8	15.3	29.0		3.40	123		10.00	34.5	0.94		2.61	4.55	0.33	24.7		0.345
6-3-2h	3.67	790	721	10.11	125	27	74.6	1.23	29.8	14.6	35.5	1.63	5.30		1.6	1.67	60.7	1.91	3.25	5.11	2.50		12.4	0.05	0.047
6-3-2K′fgr	3.02	710	578	5.40	114	24	152.0	1.21	30.6	11.5	28.8	1.89	5.40	178	10.4	2.29	125.6	1.00	2.86	13.22	4.97	0.85	21.1	0.36	0.080
6-3-2Ifgr	3.50		698	8.84	138		137.0	1.22		21.3	50.8	1.66	6.70		3.5	1.84	112.3	1.32	4.04	6.43			15.6	0.07	0.036
Lawsonite–blueschist																									
6-2-32a	2.96	735	876	3.90	92	70	26.7	0.92		23.9	52.4	2.00	7.40	168	8.90		29.0	0.53	3.70	1.12		0.16	23.6	0.17	
6-5-68	1.63	315		1.68	41	205	13.3	0.55		9.6	19.8	0.95	2.95	101			24.2	0.57	3.11	1.39		0.13	24.6		
6-5-72	4.19	710	1282	6.80	145	49	59.0	1.40	24.0	5.3	13.5	2.00	5.20	178	19.80		42.1	1.31	2.60	11.13	2.46	0.33	21.3	1.47	
0-1-2	0.28		89	0.26	12	38	7.9	0.19	10.2	7.3	17.1	0.70	2.80	129	4.80		41.6	0.09	4.00	1.08	0.77	0.06	46.2	0.28	
7-3-1′	1.59	1075	425	2.06	61	40	33.0	0.68	31.5	15.2	31.1	0.91	3.30	129	19.10	5.29	48.5	0.62	3.63	2.17	1.05	0.26	29.6	0.61	0.170
Epidote–blueschist																									
6-2-24	2.34	810	422	2.70	73	94	26.2	1.10	24.7	6.9	15.2		1.60	133			23.8	1.69		3.80	1.06	0.20	27.0		
8-2-28	0.78	110	238	0.62	24	53	7.5	0.65	41.2	6.2	14.0	0.40	1.90	128	0.90		11.5	0.33	4.75	1.21	0.18	0.06	38.7	0.06	
7168012	2.80		685	1.30	77		15.5	0.85	20.3	17.2	36.8	1.30	5.50	128	1.30		18.2	0.24	4.23	0.90	0.76	0.12	59.2	0.04	
815812	2.40		895	2.80	64	54	12.9	0.87	19.7	12.2	27.2	1.60	4.10		0.90		14.8	0.68	2.56	1.06	0.65		22.9	0.03	
714801	1.50		357	0.78	42	73	8.8	0.68	11.6	7.3	14.6	0.70	1.30		0.20		12.9	0.60	1.86	1.21	0.76		53.8	0.01	
8-2-24	0.40	65	401	0.62	33	167	15.3	0.34	20.6	12.7	27.8		3.70	122			45.0	0.17		1.20	0.74	0.13	53.2		
6-2-27a	0.74	180	248	0.78	27	138	11.7	0.47	26.8	15.6	31.5		2.90	108			24.9	0.27		0.75	0.44	0.11	34.6		
8-2-33	1.50	170	228	1.24	32		19.0	0.58	25.3	8.2	17.4	0.77	2.70				32.8	0.46	3.51	2.32	0.75		25.8		
328-4A	2.08	313	657	2.21	59	311	14.6	1.07		12.0	25.3	1.23	5.50	122		0.14	13.6	0.40	4.47	1.22		0.12	26.7		0.006
328-1C	3.20	194	547	0.57	72	152	53.0	0.69		13.4	28.4	0.99	2.40	139		0.23	76.8	0.24	2.42	3.96		0.38	126.3		0.008
329-4A	1.82	592	367	0.38	46	373	10.0	0.69		8.6	18.3	0.69	1.60	104		0.19	14.5	0.24	2.32	1.16		0.10	121.1		0.010
Epidote–amphibolite																									
6-3-41′	5.47	740	2001	1.60	167	318	32.0	4.10	29.7	11.3	24.3	1.90	9.10	122			7.8	0.18	4.79	2.83	1.08	0.26	104.4		
6-3-41″	0.74	90	1291	0.63	20	61	5.5	0.56	25.3	13.5	23.0	2.00	2.30	85			9.8	0.27	1.15	0.41	0.22	0.06	31.7		
7-3-43	2.17	230	581	0.63	67	79	29.5	0.85	19.3	16.3	34.5				0.30		34.7			1.81	1.53		106.3	0.01	
6-3-54	2.12	180	588	1.00	64	44	16.7	0.80	15.1	10.5	22.3	0.90	3.70	123	0.40		20.9	0.27	4.11	1.59	1.11	0.14	64.0	0.02	
7-3-45	0.07	30		0.60	10	68	1.3	0.30	5.9	17.3	33.6	1.50	3.50	110			4.3	0.17	2.33	0.08	0.22	0.01	16.7		
6-3-53′	2.70	265	746	3.40	80	327	18.6	1.10	18.6	6.1	13.5		5.10	141			16.9	0.67		3.05	1.00	0.13	23.5		
Amphibolite																									
6-3-25a	1.50	65	624	0.59	54	108	8.5	0.43		24.4	51.8	1.19	7.80		1.70	0.19	19.8	0.08	6.55	0.35			91.5	0.03	0.004
7-2-21msa	2.68	150	837	2.20	124	115	18.5	0.45	25.5	16.5	37.7	1.00	8.30	146	0.70		41.1	0.27	8.30	1.12	0.73	0.13	56.4	0.02	
8-1-03	2.84	160	1342	1.00	112	127	19.0	0.41	25.0	21.8	51.6	1.10	12.40	208	0.30		46.3	0.08	11.27	0.87	0.76	0.09	112.0	0.01	
CAMS [c]	0.78	260	560	2.73	75	259	12.3	1.10	15.8	19.0	39.7	1.24	7.00	181			11.2	0.39	5.65	0.65	0.78	0.07	27.5		
CAMS2 [c]	1.98	35	400	0.53	27	341	12.9	0.67	12.2	17.6	34.9	0.70	5.20	146			19.3	0.10	7.43	0.73	1.06	0.09	50.9		
6-3-25b	1.58	60	488	0.53	45	326	8.8	0.72	13.4	22.0	49.4	1.22	6.70	150			12.2	0.08	5.49	0.40	0.66	0.06	84.9		
6-5-63	3.20	110	491	0.60	44	246	5.4	0.61	12.2	19.2	37.7	1.33	6.80	169		0.29	8.9	0.09	5.11	0.28	0.44	0.03	73.3		0.008
608-1B	2.20	165	553	1.58	63	188	23.2	1.15		19.2	38.3	0.71	6.50	623		0.13	20.2	0.24	9.15	1.21		0.04	39.9		0.003
Q-1	2.87	205	835	1.21	85	187	20.7	0.80		24.2	47.1	1.24	7.80	188		0.11	25.9	0.16	6.29	0.86		0.11	70.2		0.002
GB-1	3.21	323	1110	2.32	114	186	22.3	0.70		30.7	58.0	1.49	13.00	278		0.14	31.9	0.18	8.72	0.73		0.08	49.1		0.002

[a] Reported in wt.%
[b] See discussions by Bebout et al. [24].
[c] Data from Sorensen and Grossman [39].

were determined using the inductively coupled plasma emission spectrometer (ICP) at the Department of Terrestrial Magnetism/Geophysical Laboratory (DTM/GL) of the Carnegie Institution of Washington, and the direct current plasma spectrometer (DCP) at the University of South Florida (USF); for descriptions of methods, see [30–32]. Analytical precision for the techniques is ±5% for Be and Li; for B, precision is ±5% at concentrations >10 ppm and ±10% for concentrations <10 ppm. Whole-rock data for most trace elements used in this study (Table 1) were obtained by instrumental neutron activation analysis (INAA; analyzed at Oregon State University Radiation Center under the Reactor Sharing Program). Accuracy and precision of the INAA analyses were monitored through replicate analyses of multiple standards and monitors; precision for all elements is ±15% or better. Elements for which analyses were less precise (±5–15%) include Zr, Sr, Ba, and U. Some Ba and Sr data and major element data for most samples were collected by plasma spectrometry at DTM/GL and at USF using standard $LiBO_2$ fluxed fusion techniques.

Mineral analyses for B, Cs, Rb, Sr, and Ba were obtained using the Cameca ims-4f ion microprobe at the University of Edinburgh (A.E. Bebout, G.E. Bebout, and C.M. Graham, manuscript in preparation; see Moran [31] for detailed description of analytical conditions, uncertainties, and data reduction). Thin-sectioned samples were sputtered with a primary negative $^{16}O^-$ beam (∼15 μm in diameter, 8 nA current), and secondary positive ions of B, Rb, Cs, and Ba were accelerated (4500 eV) into the mass spectrometer, separated (mass resolution ∼300), energy filtered (to remove molecular species), and counted. Spots for these analyses were in grains previously analyzed for major elements using an electron microprobe, with peak counting on ^{30}Si, ^{11}B,^{85}Rb, ^{133}Cs, and ^{138}Ba. Relative ion intensities of each element were calculated relative to Si; concentrations were calculated from the raw data by assuming that the relative ion yield for the element in the standard (NBS610 standard glass; [33]) equals the relative ion yield for the element in the unknown. In general, the major source of error in the analyses is related to sample heterogeneity (within mineral grains and between similar grains in a rock), rather than to instrumental (counting) errors. Errors based on counting statistics vary with the number of counts, and thus with the sensitivity of the element. Approximate counting errors in percent are (at the 1 and 500 ppm levels, respectively): for B, Ba, and Rb (2–4 and 0.2–0.3); for Cs (5–7 and 0.4). Ion probe accuracy, which depends on standardization and matrix effects, is likely to be worse than the counting errors; however, relative precision is likely within the counting errors. Data for relative differences in concentration between analyses in the same phase (e.g., for white-mica over a range in metamorphic grade) should be particularly usable.

3. Results

In the Catalina Schist metasedimentary rocks, devolatilization reactions released H_2O-rich C–O–H–S–N fluids [3,27,34]. H_2O contents in the rocks decrease from 3–5 wt.% in the lowest-grade, lawsonite–albite-facies rocks to 1–3 wt.% in the highest-grade, amphibolite-facies rocks; at all grades, more aluminous rocks have the highest H_2O contents [3]. This loss is attributable to breakdown of chlorite and phengitic white mica to stabilize muscovite-, biotite-, garnet-, and kyanite-bearing mineral assemblages (for generalized reactions see [24,34]). The highest-grade, amphibolite-facies metasedimentary rocks are believed to have experienced H_2O-saturated partial melting resulting in the production of quartz + plagioclase ± muscovite leucosomes and pegmatites [27]; their volatile and trace element concentrations thus reflect the combined effects of subsolidus devolatilization and partial melting. Fig. 2 summarizes the mineralogy and mineral chemistry in metasedimentary rocks in the Catalina Schist; at each grade, rocks show large variations in the modal proportions of these minerals (reflected in varying major element contents). Increases in $\delta^{15}N$ and decreases in N concentration in the higher-grade rocks relative to their likely seafloor sediment protoliths are consistent with devolatilization and loss, to fluids, of N_2 with $\delta^{15}N$ lower than that of the rocks (Table 1; Fig. 3c), perhaps during a devolatilization process approximating Rayleigh distillation [34]. It is important to note that the lower-grade rocks, because of their contrasting prograde P–T paths relative to the high-grade rocks

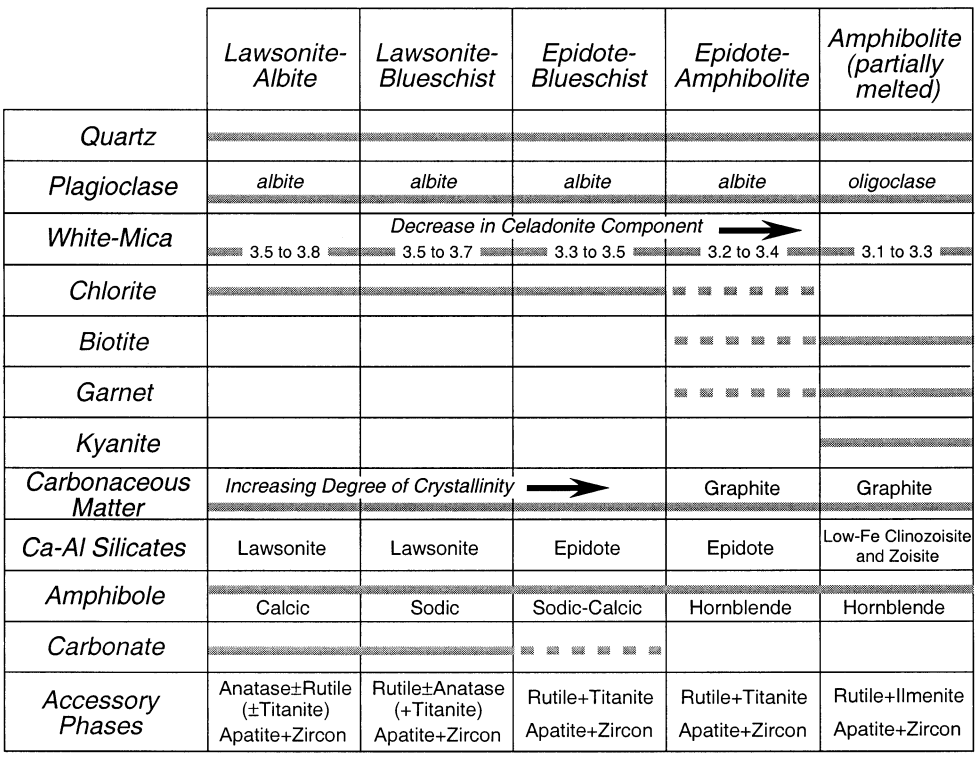

Fig. 2. Summary of mineral assemblages and mineral chemistry and textures in metasedimentary rocks of varying metamorphic grades in the Catalina Schist. Mineral assemblage information from [26,39,64,65]. For white micas, total Si atoms per formula unit (based on 11 oxygens) are given (see [26]). Carbonaceous matter in low-grade rocks (at grades if less than epidote–blueschist) is poorly crystalline material, whereas in the higher-grade rocks, it is more graphitic in structure [65]. The carbonaceous matter shows shift in $\delta^{13}C$ which correlates with N-isotope shifts and the trends in trace element compositions in this paper (C and N isotope and C/N data in [3]).

(Fig. 1), are not directly representative of the earlier stages of devolatilization of the higher-grade rocks. However, the lowest-grade (lawsonite–albite-facies) metasedimentary rocks in the Catalina Schist are broadly similar, in volatile contents and major and trace element compositions, to seafloor sediments in modern trench settings (Fig. 3; [3,24,34]) and are used as a proxy for the protoliths of the higher-grade metasedimentary rocks.

The concentrations of some other trace elements are also depleted at higher metamorphic grades (Table 1; Fig. 3). Boron, Cs, Sb, and As display decreases in mean concentration and in the range of concentrations with increasing grade (i.e., the highest-grade rocks have lower concentrations and show less variation in concentration than the lowest-grade rocks). The losses inferred by comparison of mean concentrations of the lawsonite–albite and higher-grade equivalents are in some cases dramatic (Table 1; Fig. 3). For example, mean B abundances decrease from 92 ppm ($1\sigma = 53$ ppm; $n = 10$) for lawsonite–albite rocks to 15 ppm ($1\sigma = 6.4$ ppm; $n = 10$) for amphibolite-grade equivalents, implying a possible B loss of ~85% during prograde metamorphism (Fig. 3b; [24]; cf. similar estimates of B loss with increasing metamorphism by [23]). Similarly, mean Cs contents decrease from 5.8 ppm ($1\sigma = 2.6$ ppm; $n = 10$) to 1.3 ppm ($1\sigma = 0.8$ ppm; Fig. 3a), and mean As concentrations decrease from 5.9 ppm ($1\sigma = 3.6$ ppm; $n = 7$; the value of 62 ppm for sample 9-1-33 is not included in this calculation) to 0.9 ppm ($1\sigma = 0.7$ ppm; $n = 3$), perhaps implying ~80–85% loss of Cs and As (Fig. 3a,d). Although fewer data exist for Sb, mean concentrations decrease from 3.4 ppm ($1\sigma = 2.9$ ppm; $n = 7$) to 0.17 ppm ($1\sigma = 0.07$ ppm; $n = 5$), also indicat-

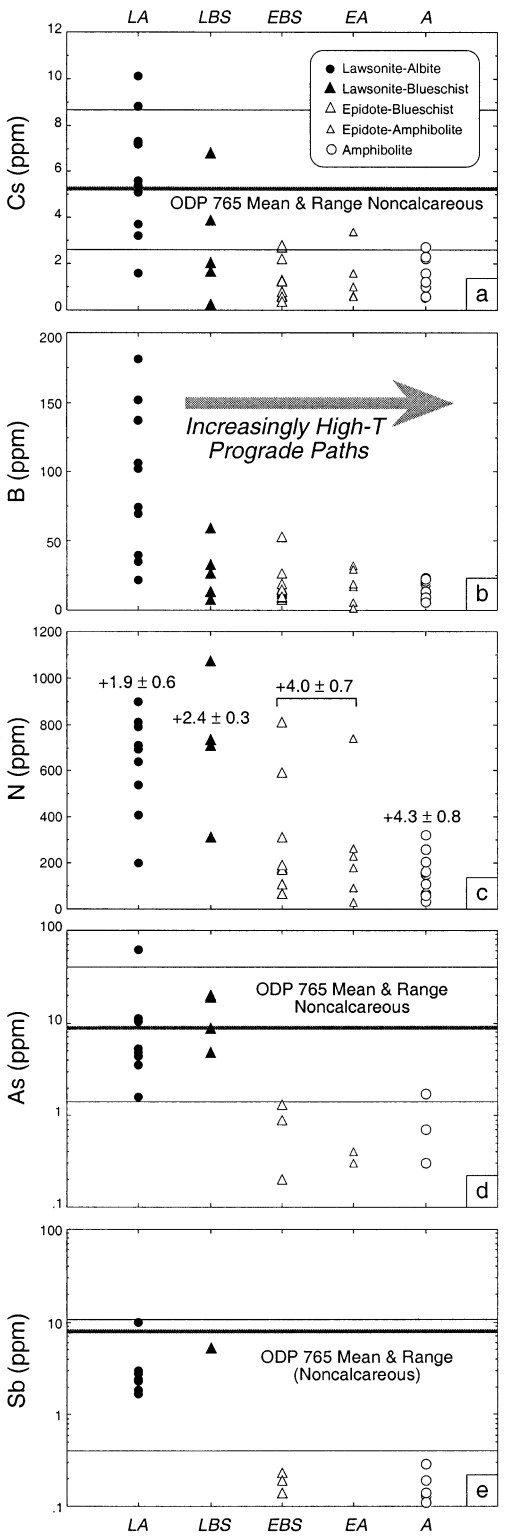

Fig. 3. (a–e) Evidence for reduction in the concentrations of Cs, B, N, As, and Sb in metasedimentary rocks of the Catalina Schist having experienced relatively high-T prograde P–T–t histories (see Fig. 1). Note the similarity of the concentrations in the lowest-grade, lawsonite–albite-facies metasedimentary rocks to the average concentrations of Cs, As, and Sb in the noncalcareous seafloor sediments from the ODP Leg 765 core (see [4]). Mean $\delta^{15}N$ values (and 1σ, relative to atmospheric N_2; from [34]) are provided for each grade in (c).

ing possible dramatic losses (perhaps >90% of the initial Sb; Fig. 3e). An incomplete Li dataset (Table 1) shows significant variation in Li concentration at single grades, and some possible minor decrease in mean Li concentrations with increasing metamorphic grade (for the lower three grades combined, mean Li concentration is 26.2 ppm [$1\sigma = 10.1$ ppm; $n = 18$]; for the two highest grades, mean Li concentration is 18.2 ppm [$1\sigma = 7.0$ ppm; $n = 12$]). Assessing whether or not the metasedimentary samples are changed in their whole-rock major element compositions during prograde metamorphism and devolatilization is complicated by the large degree of variability in composition at any one grade (cf. [35,36]). The whole-rock metasedimentary samples of the Catalina Schist do not show obvious trends of decreasing SiO_2/TiO_2 or SiO_2/Al_2O_3 (or ratios of other major oxides to TiO_2 and Al_2O_3) proposed, in other studies, to decrease with increasing grade (cf. [35]; **see EPSL Online Background Dataset** [2]).

Ion microprobe and bulk analyses of the principal metamorphic minerals indicate that B and Cs (and other LILE) are largely hosted by the micas in the metasedimentary rocks (Fig. 4; [24,31,37]). For four metasedimentary samples of epidote–blueschist and epidote–amphibolite grades, white mica is more enriched in B, Cs, Rb, and Ba than the whole-rock samples. In sample 7-3-43, the biotite is depleted in B, Rb, and Ba relative to the coexisting white mica, but is enriched in Cs relative to the white mica. Plagioclase in sample 6-3-54 is more enriched in Ba than the plagioclase in the other three samples. The concentrations of B, Cs, Rb, and Ba in chlorite, epidote, and amphibole are considerably lower. Arsenic and Sb are most likely hosted by the oxides

[2] http://www.elsevier.nl/locate/epsl, mirror site: http://www.elsevier.com/locate/epsl

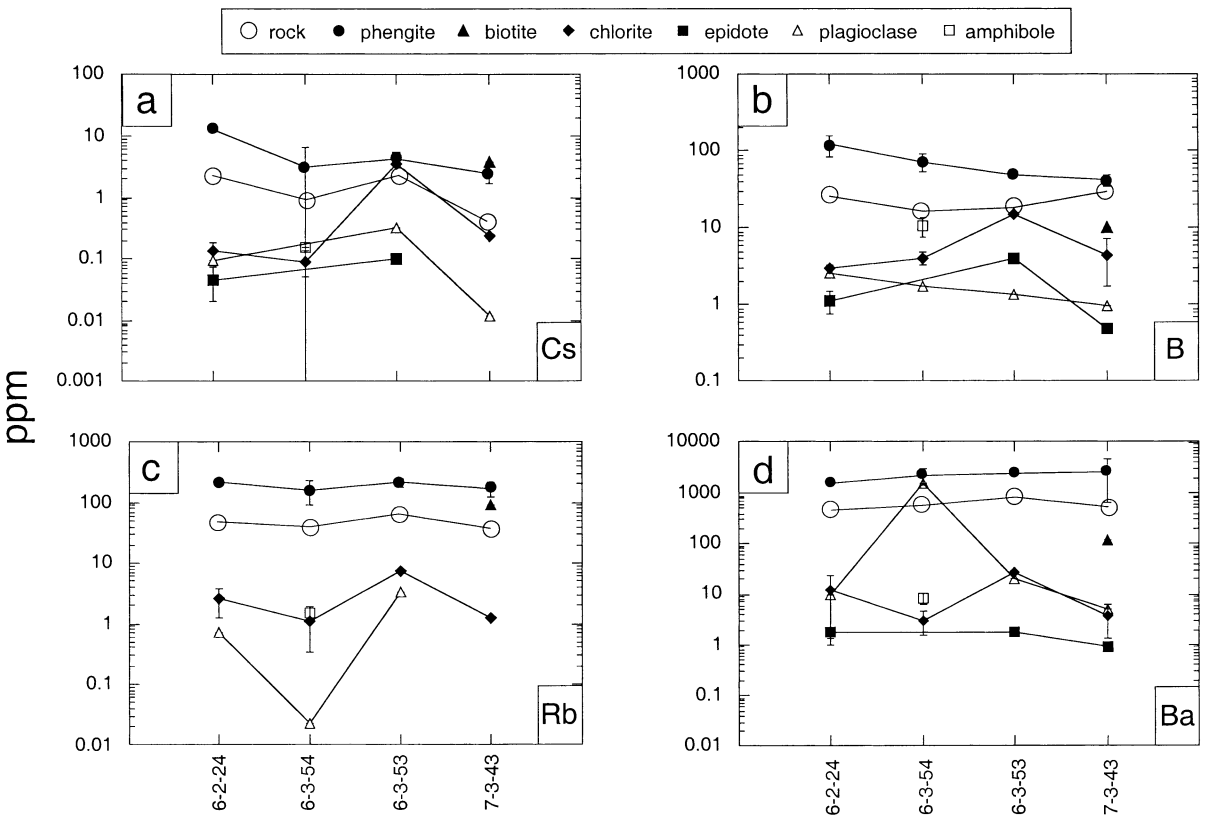

Fig. 4. (a–d) Ion microprobe B and LILE data for coexisting minerals in one epidote–blueschist-facies metasedimentary rock (sample 6-2-24) and three epidote–amphibolite-facies metasedimentary rocks (samples 6-3-54, 6-3-53, and 7-3-43) of the Catalina Schist (ion probe data are from [31]). In each of these samples, these elements are strongly enriched in micas (primarily white mica). The residency of Sr in these rocks strongly differs from that of B, Cs, Rb, and Ba, as Sr is also hosted by clinozoisite, and in lowest-grade rocks, small amounts of carbonate (see Fig. 2). Lines connecting data for the same mineral in the four rocks emphasize the systematic nature of the trace element distributions.

and sulfides in the metasedimentary rocks [11,38]. Uranium and thorium, and the REE, are expected to reside largely in accessory phases such as zircon, apatite, and titanite. In the high-grade rocks, garnet, clinozoisite, and zoisite may be important sites for the REE (cf. [39]).

The effects of varying bulk composition on whole-rock trace element concentration can be examined by comparison of the trace element contents of samples of similar grade if the varying K_2O contents (Table 1), which primarily reflect varying shale–sandstone proportions, are taken into account. At any single metamorphic grade, whole-rock K_2O contents correlate with the concentrations of B, Cs, N, Rb, and Ba, reflecting the principal residence of these trace elements in micas (the only significant K_2O-bearing mineral in the rocks; Fig. 5; seafloor sediment data in [6]). However, whole-rock Cs/K_2O and B/K_2O (presumably related directly to the concentrations of these trace elements in the micas) are dramatically lower in the epidote–amphibolite- and amphibolite-facies rocks than in the lower-grade equivalents (as reflected by the slopes of the lines on Fig. 5a,b). In contrast with this behavior, K, Ba, and Rb (hosted in micas) and Sr (hosted in micas, but also in lawsonite and clinozoisite and, in the lowest-grade rocks, in finely disseminated carbonate; [3]) do not show obvious decreases with increasing metamorphic grade (Fig. 5c,d).

The decreases in B, Cs, As, and Sb contents result in dramatic shifts in element ratios (see Table 1; Fig. 6). Cs/Th of the metasedimentary whole-rocks

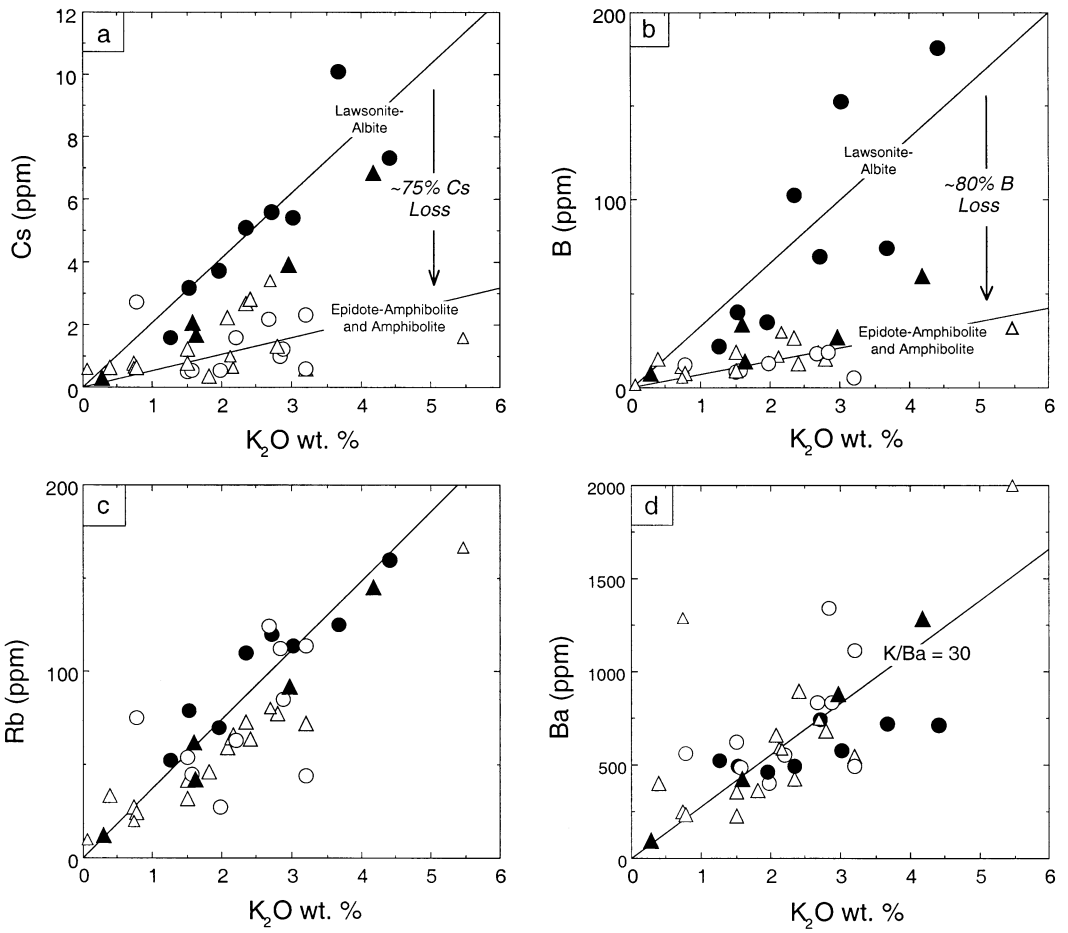

Fig. 5. (a–d) Cs–B–Rb–Ba systematics in the metasedimentary rocks of the Catalina Schist (see data in Table 1) relative to whole-rock K_2O in each of the samples. Note that the ratios of B and Cs to K_2O are lowered in the high-grade metasedimentary rocks, whereas the ratios of Rb and Ba to K_2O do not show obvious change. Particularly in the low-grade units, the concentrations of these elements correlate with whole-rock K_2O contents (Rb and Cs to a greater extent than B). Lines represent linear regressions through the data for the lowest-grade rocks (lawsonite–albite-grade samples only). For some elements (B and Cs), most of the data for the higher-grade units fall below these lines, indicating lowering of the ratios of these trace elements to K_2O during devolatilization and release of high-B/K_2O and Cs/K_2O fluids (relative to rocks). In (a) and (b), lines are estimated through the data for the highest-grade, amphibolite-facies rocks (indicating the approximate average Cs/K_2O and B/K_2O of the high-grade rocks) to demonstrate the likely magnitude of loss of Cs and B. Changes in slope of such lines drawn through the data for high- and low-grade samples (and the origin) are consistent with ~80% loss of B and ~75% loss of Cs (see similar relations demonstrated for N and K_2O by Bebout and Fogel [34]). Note that Rb/K_2O and Ba/K_2O of the higher-grade rocks, (c) and (d), do not show obvious change with increasing grade; data for all grades more strongly overlap, consistent with little effect of prograde metamorphism on these ratios. All but 6 samples have K/Rb of 200 to 500 similar to that of the ODP Site 765 sediments (see [3]; cf. [4,5]); most samples have K/Ba of 15 to 50 (line on (d) corresponds to a K/Ba of 30). The symbols are the same as those used in Fig. 3.

shows dramatic decrease over this range in grade (Fig. 6a), only in part due to the somewhat higher Th contents of the amphibolite-facies rocks (Fig. 7b), and Rb/Cs increases from ~20 (for low-grade rocks) to values approaching 120 (for high-grade rocks; Fig. 6b; also Fig. 5a,c). B/Be, B/La, and B/Li show dramatic decrease attributable to significant B loss (Table 1; Fig. 6c,d; cf. [24]). The lowest-grade, lawsonite–albite-facies rocks have relatively uniform Rb/Cs (mean = 21.3 ppm, 1σ = 5.3 ppm; Table 1; Fig. 6b) similar to that of unmetamorphosed sediments (with most seafloor sediments having Rb/Cs

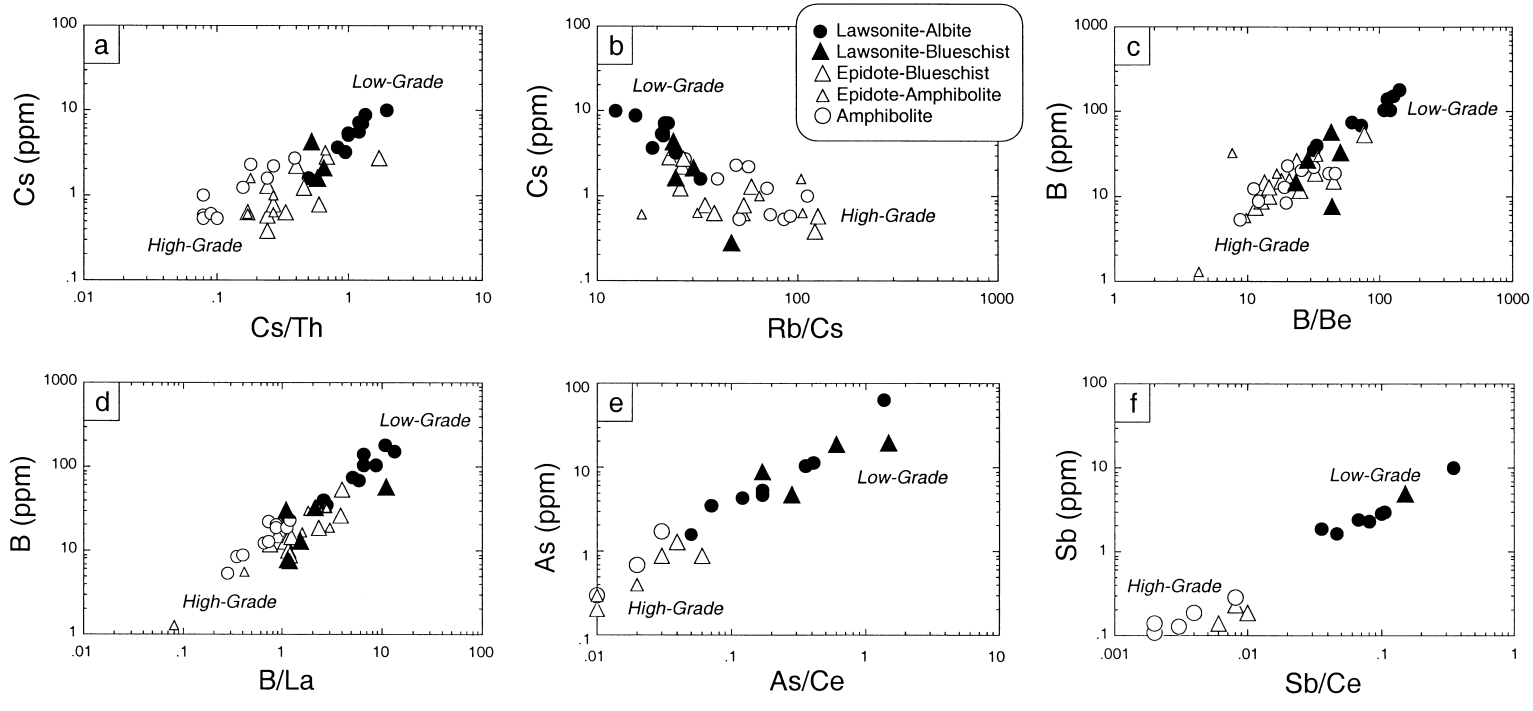

Fig. 6. (a–f) Variation in ratios among selected trace elements (B, Cs, Be, Th, Rb, La, Cs, As, and Sb) in whole-rock metasedimentary rocks of the Catalina Schist (see Table 1). The symbols are the same as those used in Fig. 3. Note that Cs/Th, Cs/Rb, B/Be, B/La, As/Ce, and Sb/Ce are all dramatically decreased in higher-grade units in the Catalina Schist. The Rb–Cs systematics differ significantly from those of the other systems as the Rb/Cs of the low-grade rocks is relatively uniform and shows greater variation in higher-grade rocks (the opposite of what is observed for the three other trace element pairs).

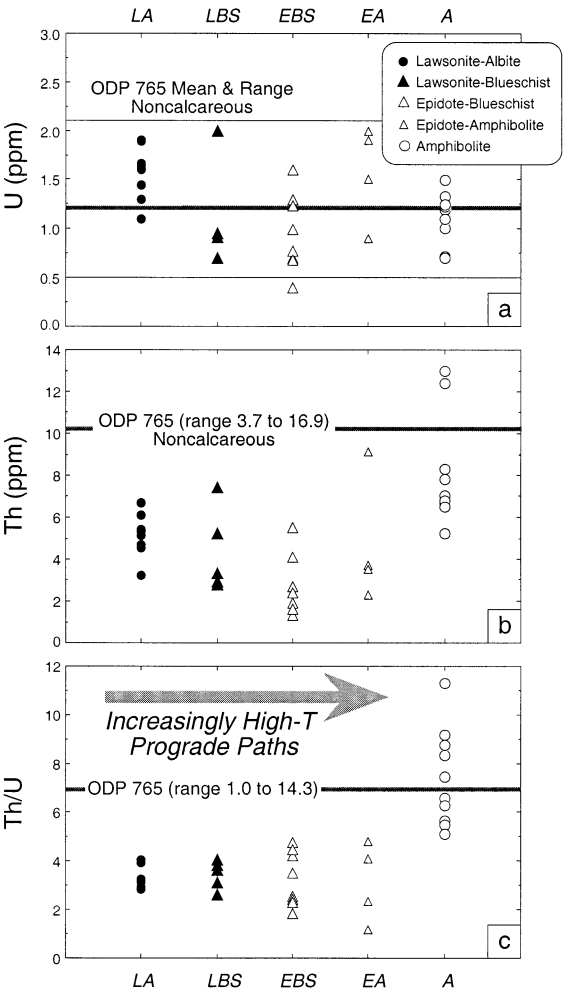

Fig. 7. (a–c) Demonstration of U–Th systmatics in the metasedimentary rocks of the Catalina Schist. Note slight statistical decrease in U ppm (a) in the higher-grade units (see text) and slight increase in the mean Th concentrations (b) of the higher-grade rocks. The two subtle trends produce an increase in the mean Th/U of the amphibolite-grade rocks (c). Ranges of U and Th concentration and Th/U for sediments in ODP core 765 (see [4]) are included for comparison (note that U and Th data from core 765 are for noncalcareous sediments only). The symbols are the same as those used in Fig. 3.

between 11 and 40; see fig. 2 in Plank and Langmuir [6] and Hart and Reid [40]), but range widely in B/Be, B/Li, B/Zr, and B/La (e.g., B/Be range of 25 to 140 for the same grade; Fig. 6c,d). Significant change is also noted in the ratios of As and Sb to the HFSE and REE (As/Ce and Sb/Ce in Table 1; Fig. 6e,f); this change is attributable to As and Sb loss, as Ce concentrations remain relatively constant.

Whether or not the U–Th systematics were disturbed by prograde devolatilization in the higher-grade units is less certain (Table 1; Fig. 7); however, some discussion of the U–Th compositions is warranted because of the possible significance of subduction-zone metamorphic processes in fractionating these elements (see [11,41]. Lawsonite–albite-facies metasedimentary rocks have mean U concentrations of 1.60 ppm ($1\sigma = 0.28$ ppm; $n = 9$), whereas amphibolite-facies equivalents have mean U contents of 1.12 ppm ($1\sigma = 0.25$ ppm; $n = 10$; Fig. 7a). The Th/U of these rocks increases with increasing grade, in large part due to the somewhat higher Th contents of the amphibolite-facies rocks (Table 1; Fig. 7b,c), with values ranging from mean Th/U of 3.28 ($1\sigma = 0.43$; $n = 9$) for lawsonite–albite-facies rocks (see similar mean values of ~4, but significant variability, for seafloor sediment in fig. 15 in Plank and Langmuir [6] and Kay and Kay [42]) to mean Th/U of 7.40 ($1\sigma = 2.0$; $n = 10$) for amphibolite-facies equivalents (Table 1).

4. Discussion

4.1. Evidence for varying trace element behavior during forearc devolatilization

The trace element systematics in the Catalina Schist metasedimentary rocks can be explained by varying degrees of element removal by fluids during devolatilization reactions, with the most depleted elements being those most strongly partitioned from the micas (for B, Cs, and N) and other minerals (perhaps the oxides and sulfides for As and Sb) into metamorphic fluids. The lower Cs/K_2O and B/K_2O in epidote–amphibolite- and amphibolite-facies rocks (Fig. 5a,b) are consistent with losses of B and Cs similar in magnitude to the loss inferred for N in the same rocks (~75% loss of N inferred by Bebout and Fogel [34]; Table 1; Fig. 3c). Preferential removal of B and Cs relative to Be, Li, Th, Rb, Zr, and La can explain the decreased B/Be, B/Li, B/La, B/Zr and Cs/Th and increased Rb/Cs (Fig. 6; Table 1). There is a weaker suggestion in the Catalina Schist data (complicated by compositional variability at each

grade and requiring further testing) that Li partitions into forearc aqueous fluids to a slightly greater extent than Be (but to a far lesser extent than B and Cs). The evolved metamorphic fluids are inferred to have had complementary, highly fractionated trace element compositions (high B/Be, B/K_2O, B/Li, B/La, B/Zr, Cs/Th, and Cs/K_2O and low Rb/Cs) relative to the rocks (Figs. 5 and 6).

For each unit, the preferential loss of fluid-mobile trace elements such as B and Cs relative to Be, Li, Th, Rb, Zr, and La was probably incremental, occurring over a broad range of pressures and temperatures during prograde metamorphism and involving continuous metamorphic reactions (cf. [24,34]). These reactions involved progressive changes in the compositions of minerals such as mica and chlorite (e.g., decreases in the phengite component in white micas) without marked decrease in the modal proportions of mica. To a lesser extent, minor breakdown of chlorite and the white micas resulted in the appearance of phases such as biotite, kyanite, and garnet (Fig. 2). Thus, the decreases in whole-rock contents of elements hosted in the micas largely reflect the progressive reequilibration of the micas with metamorphic fluids (i.e., repeated fluid–mineral trace element partitioning with successive 'batches' of fluid) rather than breakdown of the micas (primarily white micas) to produce other potassic phases such as potassium feldspar (which is absent in the metasedimentary rocks of all grades). In these rocks, the Rb/Cs systematics (Fig. 6b) most directly reflect the effects of progressive fluid–mica partitioning, as both elements are primarily hosted by the micas (Fig. 4). In contrast, the Cs/Th and B/La systematics (Fig. 6a,d) are impacted by both the changes in mica B and Cs contents with increasing metamorphic grade and varying relative abundances of the micas and Th- and La-rich phases at each grade. The decreases in whole-rock Cs/Th and B/La are primarily the result of dramatic Cs and B loss, largely from the micas (Fig. 3a,b, Figs. 4–6a,d). The B/Be systematics differ from those of the other systems in that Be is more uniformly distributed among the silicate phases in the metasedimentary samples, occurring at significant concentrations in the micas (Fig. 6c; [24,37]). In a detailed ion microprobe study of the trace element concentrations in mineral phases in the Catalina Schist metasedimentary rocks, A.E. Bebout, G.E. Bebout, and C.M. Graham (in prep.) demonstrated (1) that the concentrations of B and Cs in white-mica show decreases with increasing metamorphic grade which parallel the whole-rock variations (in contrast, Ba and Rb concentrations in the micas show no decrease with increasing grade), and (2) that the whole-rock concentrations of the B, Cs, Rb, and Ba can be roughly reproduced using the mineral concentrations and mineral modes in these rocks. Thus, the whole-rock variations in trace element concentration appear to reflect the effects of prograde recrystallization and mineral–fluid partitioning rather than other processes such as retrograde enrichment.

The extent to which trace elements were fractionated by fluid–rock partitioning depended on factors such as the amount of local fluid loss, which in turn depended on the chemical composition of the rocks. Degrees of fluid–rock interaction, involving either locally or externally derived fluid, and the P- and T-dependent fluid–mineral partition coefficients for these elements, may thus dictate the degrees of depletion of fluid-mobile elements during prograde metamorphism (see [24] for calculations and discussion). The enhanced partitioning of B, Cs, As, and Sb (relative to Be, Li, Rb, the HFSE, and the REE) into metamorphic fluids inferred from this study is, in general, compatible with the results of experimental and other field-based studies of element fluid–mineral partitioning and mobility (see [15,17,43–49]). The abundances and compositions of micas in the metasedimentary rocks of the Catalina Schist strongly control the whole-rock abundances of N, B, Cs, Rb, and the other LILE (Fig. 4; cf. [24,31,37,50]). Ion microprobe data demonstrate that B and the LILE in metamorphosed mafic rocks are also hosted primarily by muscovite and biotite [31,37]. Thus, the stability relations (and solubilities) of the micas may govern the release of these elements from the subducting slab (see [24,37,51]). The data for amphibolite-grade metasedimentary rocks of the Catalina Schist, which are believed to have experienced water-saturated partial melting, document the retention to >650°C of significant concentrations of these elements, likely in micas. It is possible, in many subduction zones (particularly in relatively warm subduction zones; Fig. 1), that the systematics of some LILE, B, Be, and Li in subducted argillaceous sed-

iments during further prograde heating (to >650ºC) would at greater depths be impacted by dehydration–melting reactions involving breakdown of micas and production of high-Si partial melts (cf. [52]).

The mobility of siderophile/chalcophile elements such as Sb and As likely depends on the stabilities of host oxide and sulfide phases during prograde metamorphism, hence on possible desulfidation of the rocks and local oxygen fugacity relations [11]. Sulfide minerals (pyrite and pyrrhotite abundant in low-grade metasedimentary rocks) are absent or minor in abundance in higher-grade rocks (at grades of epidote–blueschist or higher), providing a possible explanation for the high degrees of removal of the chalcophile elements As and Sb in the higher-grade rocks. The partitioning of U into the metamorphic fluids would also depend critically on oxygen fugacity, with more oxidizing conditions favoring the enhanced mobility of U as U^{6+} hydroxide form [11,12,44]. Based on the abundance of graphite (which defines the maximum f_{O_2}) in all Catalina Schist metasedimentary samples, and the existing knowledge of fluid compositions for the suite (>90 mole% H_2O at all grades), oxygen fugacity is regarded as having been near the QFM (quartz–magnetite–fayalite) buffer (over the range of 400–600ºC at 10 kbar, f_{O_2} of ~1 log unit above QFM at lower temperatures, to ~2 log units below QFM at the higher temperatures; [53]). This f_{O_2} range is likely to have been sufficiently reducing to stabilize U^{4+}, known to partition to a lesser extent than U^{6+} into fluids and melts relative to minerals [45], as the dominant U complex. The apparent relative immobility of U in the metamorphic fluids, as deduced by the lack of obvious evidence for loss of U from rocks at the higher grades (Fig. 7), can be explained by the complexing of U predominantly as the more mineral-compatible U^{4+}. Regarding other possible effects on the whole-rock U–Th compositions, metasedimentary rocks of all grades contain varying amounts of zircon and apatite (both known to incorporate U and Th); however, the modal abundances of clinozoisite/zoisite (lawsonite–albite and lawsonite–blueschist rocks contain lawsonite as the Ca–Al–silicate phase; Fig. 2) appear to be lower in amphibolite-facies rocks, perhaps providing one explanation for the altered Th/U of the highest-grade rocks (cf. [39]). Perhaps more likely, the stability of titanite (sphene) could have played a key role in the whole-rock U–Th systematics–titanite (which can host REE, U, and Th; [39]) is present in metasedimentary rocks at lower grades, but absent and replaced by rutile (with ilmenite) as the dominant TiO_2 phase in amphibolite-facies rocks.

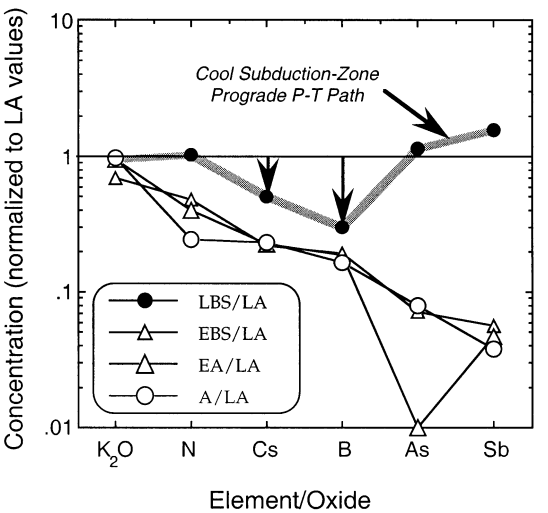

Fig. 8. Plot of mean element concentrations in lawsonite–blueschist (*LBS*), epidote–blueschist (*EBS*), epidote–amphibolite (*EA*), and amphibolite (*A*) facies metasedimentary rocks normalized to the concentrations of the same components in lawsonite–albite (*LA*) facies metasedimentary rocks, showing apparent varying susceptibilities of the components to depletion during metamorphism along increasingly higher-T prograde P–T paths (see inferred prograde paths for the various units in fig. 1 from [26]). Note that the comparison of the LBS to the LA metasedimentary rocks (broader line) indicates preferential depletion of Cs and B relative to K_2O, N, As, and Sb along a relatively low-T prograde metamorphic path (see text for discussion).

The data for the relatively 'fluid-mobile' trace elements may reflect varying susceptibilities to loss during devolatilization along increasingly higher-temperature P–T paths in the Catalina subduction zone (Fig. 8). In Fig. 8, the volatile contents of each of the higher-grade units of the Catalina Schist are compared with the volatile contents of the lawsonite–albite-grade rocks, which are similar in their volatile and trace element contents and stable isotope compositions to likely unmetamorphosed equivalents. Perhaps the most interesting comparison is that of the lawsonite–blueschist-grade rocks with the lawsonite–albite-grade rocks (indicated by the bolder line). From this comparison, it is evident that

B and Cs were depleted to a greater degree than N, As, and Sb during prograde metamorphism along the relatively low-temperature $P–T$ path experienced by the lawsonite–blueschist-facies rocks (vertical arrows on Fig. 8). Furthermore, the magnitudes of loss for B and Cs appear to differ significantly (~70% loss for B; ~50% for Cs). Higher-grade units show dramatic losses of all five of the elements. However, B, Cs, and N are retained at significant concentrations in even the amphibolite-facies metasedimentary rocks because of the continued stability of micas (largely muscovite) at high grades.

4.2. Implications of trace element fractionation during devolatilization in forearcs

Subduction-zone metamorphism should result in the development of a variety of geochemical reservoirs related to the release of slab fluids (i.e., hydrous fluids, silicate liquids), the mobilization of these fluids at various depths in forearc and subarc regions, and the transport of devolatilized, chemically fractionated slabs into the deep mantle [3,14]. Evidence for devolatilization, fluid transport, and metasomatism in the Catalina Schist (this study; [3,24,27,34,50]) directly predicts the release and large-scale mobilization of hydrous fluids (and dissolved species) in forearc regions, particularly in relatively warm subduction zones. Attempts to trace 'deep-sourced' fluid contributions (i.e., not merely compaction-related) in shallow accretionary prisms have been inconclusive [16]. However, recent geochemical studies of clasts, muds, and low-chlorinity fluids from actively venting forearc serpentinite seamounts [13–15] have revealed fractionated fluid elemental abundance patterns in the solids (e.g., strongly elevated B contents, possibly elevated contents of Cs, Rb, and Li), and C–H–O isotope fluid compositions compatible with the addition of slab-derived fluids with some chemical/isotopic similarities to the fluids released from the Catalina Schist metasedimentary rocks.

The relationships in Fig. 8 point to differing degrees of deep retention (and recycling), among trace elements, that reflect the differential fluid–mineral partitioning of these elements during forearc devolatilization and as the result of varying prograde, subduction-zone $P–T$ histories. The higher contents of fluid-mobile trace elements in the Catalina Schist metasedimentary rocks representing the lowest-T prograde paths (the lawsonite–blueschist-facies rocks; indicated by the broader line in Fig. 8) imply that, in cool subduction zones, these elements are efficiently retained in subducting sedimentary rocks to great depths where they could be available for addition to arc source regions. Further tests of these proposed varying trace element susceptibilities to forearc loss in fluids should be conducted on other high-P/T metamorphic suites, particularly on suites representing subduction to depths greater than those represented by the Catalina Schist (15–45 km).

Variations in B/Be, Cs/Th, As/Ce, and Sb/Ce among arcs from differing convergent-margin thermal regimes, and conceivably some cross-arc declines in these ratios, can be reconciled with evidence from the Catalina Schist for varying degrees of forearc element removal as a function of prograde thermal history. We suggest that the shallow devolatilization (and even melting) experienced by the higher-grade units of the Catalina Schist (i.e., epidote–amphibolite- and amphibolite-facies units) may be analogous to the processes attending forearc metamorphism in relatively warm subduction zones such as the Cascadia plate margin (cf. [54,55]). A comparison of the volatile and trace element contents of the epidote–amphibolite- and amphibolite-facies metasedimentary rocks with those of the lawsonite–albite-facies rocks (and unmetamorphosed equivalents) suggests that dramatic shallow devolatilization should occur in such subduction zones. This shallow devolatilization should result in smaller hydrous fluid fluxes beneath arcs and the production of fewer arc volcanoes [25] which erupt lavas lacking the distinctive trace element signatures of hydrous fluid additions but possessing trace element abundances consistent with additions of slab sediment melts [55]. This warmer thermal evolution is thought to be more representative of the thermal conditions in Archean subduction zones; thus, a similar devolatilization process, selectively removing relatively fluid-mobile trace elements, is likely to have affected the deep recycling of these elements in the Archean (cf. [41]).

Later-stage subduction produced the relatively cooler thermal regimes reflected by the lower-grade units of the Catalina Schist (Fig. 1) and, for the lawsonite–blueschist- and epidote–blueschist-facies

rocks, resulted in less dramatic volatile and trace element losses during subduction to the same depths. The lawsonite–blueschist-facies metasedimentary rocks are relatively similar in trace element composition to the lawsonite–albite-facies (and unmetamorphosed) equivalents (Figs. 3 and 5–7). This similarity reflects the retention of volatiles (including the fluid-mobile elements) to far greater depths at later, cooler stages in the Catalina subduction zone, perhaps for some volatiles to depths of the blueschist–eclogite transition ([56]; Fig. 1). The later-stage thermal regime of the subduction zone producing the Catalina Schist was perhaps more similar to that of the present-day Kurile, Marianas, Aleutian, and southern Alaska subduction zones (cf. [9–12,25,30,57]): that is, relatively cool, affording the addition of hydrous fluids with distinctive trace element signatures (e.g., high B/Be, B/Li, B/La, B/Zr, Cs/Th, Cs/Rb, As/Ce, and Sb/Ce) to the mantle wedge beneath the arc.

The aforementioned relationships are illustrated using representative volcanic arc data in Fig. 9, in which element ratios (Cs/Th, Rb/Cs, B/Be, B/La, As/Ce, and Sb/Ce) are plotted versus K_2O contents. Here, data are shown for a relatively warm subduction zone (Cascades) and two cooler subduction zones (Marianas and Kuriles; cf. [58,59]). For comparison, representative data (in labelled, patterned fields) are shown for oceanic island basalts (OIB) and less altered mid-ocean ridge basalts (MORB) which collectively are taken as representative of normal sub-oceanic mantle domains where there is little or no subduction contribution. Contents of K_2O generally increase toward back-arc regions and typically are correlated with progressive depletion of the 'fluid-mobile' elements (B, Cs, As, and Sb; cf. [10,14]); the across-arc trends of decreasing B, Cs, As, and Sb abundance are subdued in the relatively 'hot' Cascades arc, presumably due to the greater prior removal of these elements during relatively high-*T* forearc metamorphism. In all three arc systems (and particularly for the Cascades arc), the trace element ratios in volcanic rocks toward back-arc regions approach the ratios in OIB and unaltered MORB. Thus, the significant enrichments of B, Cs, As, and Sb in typical arc magmas can be reconciled with variably efficient transfer of these elements from subducted slabs (sediment and/or ocean crust components) to the respective arc magma sources. The fact that many of the element ratios used are not significantly fractionated by partial melting processes argues both against direct melting of the slabs and for a multi-stage process in forming arc magma sources [10,30,59]. Progressive across-arc declines in B/Be, Cs/Th, As/Ce, and Sb/Ce (e.g., as documented for the Kurile [10,11] and other arcs [9,30]; Fig. 9) are viewed as reflecting diminished inputs of hydrous slab-derived fluids, but may also indicate changes with depth in the trace element ratios of evolved metamorphic fluids and the increased impact of melt inputs from the slab (see [14,24,46]). Any shift in the stable isotope compositions of rocks during forearc devolatilization will strongly impact the stable isotope compositions of partial melts generated at higher temperatures [3,49,60].

5. Conclusions

In the Catalina Schist, the preservation of tectonometamorphic units representing a rapidly cooling subduction zone has allowed us to examine forearc devolatilization as a function of varying prograde thermal history. Such information can be directly applied to understanding the chemical evolution of present-day subduction zones of varied thermal structures, pointing to specific mass-balance experiments for individual arcs which could test the efficiency of seafloor-to-arc transfer. The trace element data for metasedimentary rocks in the Catalina Schist indicate systematics in the differential extents of element loss that can be related to the relative stabilities of the elements' mineral hosts (particularly the micas and sulfides). Our results (also see [23,24]) complement recent examinations of convergent-margin trace element mobility based on analysis of the sediments outboard of trenches, investigation of trace element and stable isotope systematics in arc volcanic rocks and serpentinite seamounts, and experimental studies of the effects of metamorphic fluid–rock interactions on the compositions of both subducting lithologies and their liberated fluid phases. A more complete understanding of the effects of devolatilization and melting on the chemical compositions of subducting slabs awaits more detailed study of trace element behavior during sub-

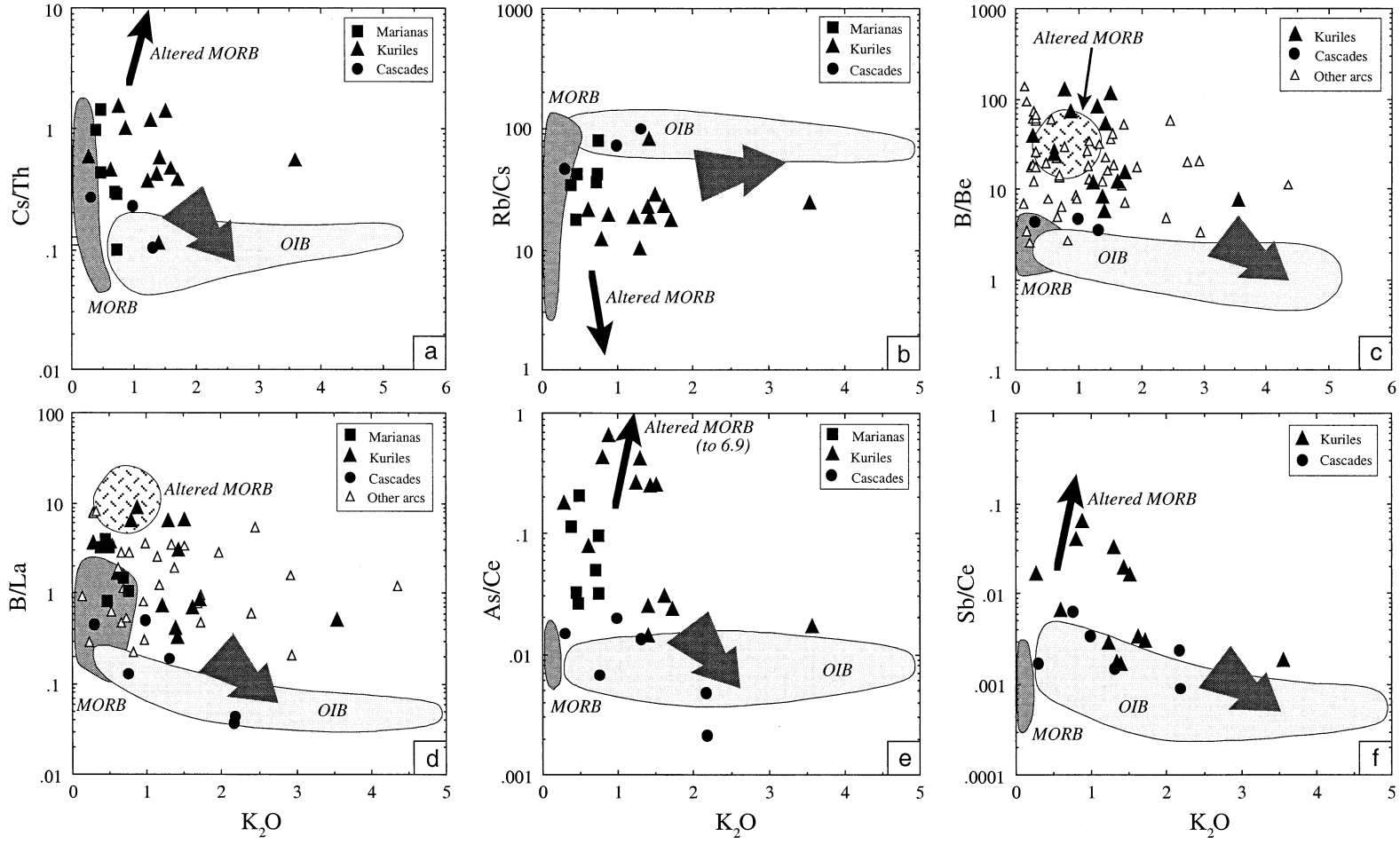

Fig. 9. (a–f) Ratios of fluid-mobile elements to other incompatible elements as a function of K_2O content (K_2O in wt.%) for selected lavas from the Kurile, Marianas, and Cascades volcanic arcs and basalts from oceanic islands (*OIB*) and mid-ocean ridges (*MORB*; less altered in shaded region). The data used are as follows. As and Sb data ([11], and [58], and references therein); Be and B: altered MORB, Marianas (W.P. Leeman, unpubl. data), Kuriles [10], Cascades [55], MORB and OIB [59,66], W.P. Leeman, unpubl. data; Rb, Cs, Th ([58], and references therein; W.P. Leeman, unpubl. data). Fat, darkly patterned arrows indicate the general trajectories of the ratios in volcanic rocks across arcs, and the finer, black arrows indicate trajectories from fresh MORB toward values for seafloor altered MORB (approximate fields shown in patterned regions in (c) and (d)). In all three of the arcs, enrichments in the fluid-mobile elements show declines with increasing K_2O content, which correlates with degrees of melting, decreasing slab inputs, and in across-arc suites, depth-to-slab. Fresh MORB and OIB tend to have similar ranges for the ratios plotted despite degree of differentiation (range in K_2O). The 'cooler' Kurile and Mariana arcs show more dramatic enrichments in the fluid-mobile elements consistent with greater additions in slab-derived 'fluids' whereas, in the 'hot' Cascades arc, enrichments in these elements (and across-arc variation in these element ratios) are smaller, consistent with the presence of a more devolatilized slab beneath the Cascades arc. Overlap of data for the Cascades with data for OIB and fresh (unaltered) MORB further confirms the similarity in the respective magma sources.

duction-zone metamorphism of metabasaltic rocks (see [51,61]). Studies of blueschist- and eclogite-facies suites representing high-P/T metamorphism at pressures greater than those represented by the Catalina Schist forearc suite (>50 km; e.g., [61,62]), and additional experimental approaches (e.g., [43–48,63]), are required to elucidate trace element behavior during devolatilization at the greater depths beneath arcs.

Devolatilization in forearc regions probably strongly influences the global budgets of trace elements such as B, Cs, As, Sb, and perhaps U (and other volatile components; e.g., H_2O, C, N; see [3]), preventing their deep subduction to varying degrees depending on the thermal evolution of the subduction zones. As the result of forearc devolatilization, these elements may be returned toward the surface in Catalina-like H_2O-rich fluids which contribute significantly to the production of forearc serpentinite seamounts and the fluid budgets in shallow parts of accretionary complexes. It should ultimately be possible to refine our understanding of these fluxes by combining information regarding thermal structure of modern subduction zones with the information regarding relative efficiency of subduction as a function of thermal history gained through study of high-P/T metamorphic suites, and with the geochemistry of the arc lavas, in studies evaluating the recycling behavior of individual elements at individual convergent margins.

Acknowledgements

We acknowledge support by NSF grants (EAR92-06679 and EAR94-05625 to GEB; EAR90-18996, EAR91-19110, and EAR94-19018 to WPL; EAR94-05404 to AEB). Special thanks are extended to the Oregon State University Reactor Sharing Program, through which we obtained the INAA data, and to Julie Morris and Fouad Tera, in whose laboratories (Department of Terrestrial Magnetism and Geophysical Laboratory, Carnegie Institution of Washington) the B–Be–Li analyses were performed. We thank Colin Graham and John Craven at the University of Edinburgh for their help in acquiring the ion microprobe data and Simon Peacock and James Brenan for their reviews. ***[CL]***

References

[1] E. Ito, D.M. Harris, A.T. Anderson Jr., Alteration of oceanic crust and geologic cycling of chlorine and water, Geochim. Cosmochim. Acta 47 (1983) 1613–1624.
[2] S.M. Peacock, Fluid processes in subduction zones, Science 248 (1990) 329–337.
[3] G.E. Bebout, The impact of subduction-zone metamorphism on mantle–ocean chemical cycling, Chem. Geol. 126 (1995) 191–218.
[4] T. Plank, J. Ludden, Geochemistry of sediments in the Argo Abyssal Plain at ODP Site 765: a continental margin reference section for sediment recycling in subduction zones, Proc. ODP, Sci. Results 123 (1992) 167–189.
[5] T. Plank, C.H. Langmuir, Tracing trace elements from sediment input to volcanic output at subduction zones, Nature 362 (1993) 739–743.
[6] T. Plank, C.H. Langmuir, The chemical composition of subducting sediment and its consequences for the crust and mantle, Chem. Geol. 145 (1998) 325–394.
[7] H. Staudigel, T. Plank, B. White, H.-U. Schmincke, Geochemical fluxes during seafloor alteration of the basaltic upper oceanic crust: DSDP Sites 417 and 418, in: G.E. Bebout, D.W. Scholl, S.H. Kirby, J.P. Platt (Eds.), Subduction: Top to Bottom, Am. Geophys. Union, Geophys. Monogr. 96 (1996) 19–38.
[8] R. von Huene, D.W. Scholl, Observations at convergent margins concerning sediment subduction, subduction erosion, and the growth of continental crust, Rev. Geophys. 29 (1991) 279–316.
[9] J.D. Morris, W.P. Leeman, F. Tera, The subducted component in island arc lavas: constraints from Be isotopes and B–Be systematics, Nature 344 (1990) 31–36.
[10] J.G. Ryan, J.D. Morris, F. Tera, W.P. Leeman, A. Tsvetkov, Cross-arc geochemical variations in the Kurile island arc as a function of slab depth, Science 270 (1995) 625–628.
[11] P.D. Noll, H.E. Newsom, W.P. Leeman, J. Ryan, The role of hydrothermal fluids in the production of subduction zone magmas: evidence from siderophile and chalcophile trace elements and boron, Geochim. Cosmochim. Acta 60 (1996) 587–611.
[12] T. Elliott, T. Plank, A. Zindler, W. White, B. Bourdon, Element transport from slab to volcanic front at the Mariana arc, J. Geophys. Res. 102 (1997) 14991–15019.
[13] P. Fryer, M. Mottl, L. Johnson, J. Haggerty, S. Phipps, H. Maekawa, Serpentine bodies in the forearcs of Western Pacific convergent margins: origin and associated fluids, in: B. Taylor, J. Natland (Eds.), Active Margins and Marginal Basins of the Western Pacific, Am. Geophys. Union, Geophys. Monogr. 88 (1995) 259–279.
[14] J. Ryan, J. Morris, G. Bebout, B. Leeman, F. Tera, Describing chemical fluxes in subduction zones: insights from 'depth-profiling' studies of arc and forearc rocks, in: G.E. Bebout, D.W. Scholl, S.H. Kirby, J.P. Platt (Eds.), Subduction: Top to Bottom, Am. Geophys. Union Geophys. Monogr. 96 (1996) 263–268.
[15] L.D. Benton, Origin and Evolution of Serpentine Seamount

Fluids, Mariana and Izu–Bonin Forearcs: Implications for the Recycling of Subducted Material, Ph.D. Diss., Univ. Tulsa, OK, 1997, 209 pp.
[16] M. Kastner, H. Elderfield, J.B. Martin, Fluids in convergent margins: what do we know about their composition, origin, role in diagenesis and importance for oceanic chemical fluxes?, Philos. Trans. R. Soc. London 335 (1991) 243–259.
[17] C.F. You, P.R. Castillo, J.M. Gieskes, L.H. Chan, A.J. Spivack, Trace element behavior in hydrothermal experiments: implications for fluid processes at shallow depths in subduction zones, Earth Planet. Sci. Lett. 140 (1996) 41–52.
[18] U. Tsunogai, J. Ishibashi, H. Wakita, T. Gamo, T. Masuzawa, T. Nakatsuka, Y. Nojiri, T. Nakamura, Fresh water seepage and pore water recycling on the seafloor: Sagami Trough subduction zone, Japan, Earth Planet. Sci. Lett. 138 (1996) 157–168.
[19] G.E. Bebout, Volatile transfer and recycling at convergent margins: mass-balance and insights from high-P/T metamorphic rocks, in: G.E. Bebout, D.W. Scholl, S.H. Kirby, J.P. Platt (Eds.), Subduction: Top to Bottom, Am. Geophys. Union, Geophys. Monogr. 96 (1996) 179–193.
[20] D. Abbott, M. Lyle, Age of oceanic plates at subduction and volatile recycling, Geophys. Res. Lett. 11 (1984) 951–954.
[21] G.E. Bebout, Field-based evidence for devolatilization in subduction zones: implications for arc magmatism, Science 251 (1991) 413–416.
[22] H. Staudigel, S.D. King, Ultrafast subduction: the key to slab recycling efficiency and mantle differentiation?, Earth Planet. Sci. Lett. 109 (1992) 517–530.
[23] A.E. Moran, V.B. Sisson, W.P. Leeman, Boron depletion during progressive metamorphism: implications for subduction processes, Earth Planet. Sci. Lett. 111 (1992) 331–349.
[24] G.E. Bebout, J.G. Ryan, W.P. Leeman, B–Be systematics in subduction-related metamorphic rocks: characterization of the subducted component, Geochim. Cosmochim. Acta 57 (1993) 2227–2237.
[25] S. Kirby, E.R. Engdahl, R. Denlinger, Intraslab earthquakes and arc volcanism: dual expressions of crustal and upper mantle metamorphism in subducting slabs, in: G.E. Bebout, D.W. Scholl, S.H. Kirby, J.P. Platt (Eds.), Subduction: Top to Bottom, Am. Geophys. Union, Geophys. Monogr. 96 (1996) 195–214.
[26] M. Grove, G.E. Bebout, Cretaceous tectonic evolution of coastal southern California: insights from the Catalina Schist, Tectonics 14 (1995) 1290–1308.
[27] G.E. Bebout, M.D. Barton, Metasomatism during subduction: products and possible paths in the Catalina Schist, California, Chem. Geol. 108 (1993) 61–92.
[28] E.H. Bailey, W.P. Irwin, D.L. Jones, Franciscan and related rocks. Calif. Dep. Mines Geol. Bull. 183 (1964).
[29] D.K. Rea, L.J. Ruff, Composition and mass flux of sedimentary materials entering the World's subduction zones: implications for global sediment budgets, great earthquakes, and volcanism, Earth Planet. Sci. Lett. 140 (1996) 1–12.
[30] J.G. Ryan, C.H. Langmuir, The systematics of boron abundances in young volcanic rocks, Geochim. Cosmochim. Acta 57 (1993) 1489–1498.
[31] A.E. Moran, The Effect of Metamorphism on the Trace Element Composition of Subducted Oceanic Crust and Sediment, Ph.D. Diss., Rice Univ., Houston, TX, 1993, 367 pp.
[32] J.G. Ryan, C.H. Langmuir, The systematics of lithium abundances in young volcanic rocks, Geochim. Cosmochim. Acta 51 (1987) 1727–1741.
[33] R.W. Hinton, Ion microprobe trace element analysis of silicates: measurement of multi-element glasses, Chem. Geol. 83 (1990) 11–25.
[34] G.E. Bebout, M.L. Fogel, Nitrogen-isotope compositions of metasedimentary rocks in the Catalina Schist, California: implications for metamorphic devolatilization history, Geochim. Cosmochim. Acta 56 (1992) 2839–2849.
[35] J. Ague, Mass transfer during Barrovian metamorphism of pelites, south-central Connecticut, I, evidence for changes in composition and volume, Am. J. Sci. 294 (1994) 989–1057.
[36] B.P. Roser, S. Nathan, An evaluation of elemental mobility during metamorphism of a turbidite sequence (Greenland Group, New Zealand), Geol. Mag. 134 (1997) 219–234.
[37] K.J. Domanik, R.L. Hervig, S.M. Peacock, Beryllium and boron in subduction zone minerals: an ion microprobe study, Geochim. Cosmochim. Acta 57 (1993) 4997–5010.
[38] K.H. Wedepohl (Ed.), Handbook of Geochemistry, Vols. II-1–II-5, Springer, New York, 1978.
[39] S.S. Sorensen, J.N. Grossman, Enrichment of trace elements in garnet amphibolites from a paleo-subduction zone: Catalina Schist, southern California, Geochim. Cosmochim. Acta 53 (1989) 3155–3177.
[40] S.R. Hart, M.R. Reid, Rb/Cs fractionation: a link between granulite metamorphism and the S-process, Geochim. Cosmochim. Acta 55 (1991) 2379–2383.
[41] M.T. McCulloch, The role of subducted slabs in an evolving earth, Earth Planet. Sci. Lett. 115 (1993) 89–100.
[42] R.W. Kay, S.M. Kay, Crustal recycling and the Aleutian arc, Geochim. Cosmochim. Acta 52 (1988) 1354–1359.
[43] Y. Tatsumi, D.L. Hamilton, R.W. Nesbitt, Chemical characteristics of fluid phase released from a subducted lithosphere and origin of arc magmas: evidence from high-pressure experiments and natural rocks, J. Volcanol. Geotherm. Res. 29 (1986) 293–309.
[44] J.M. Brenan, H.F. Shaw, D.L. Phinney, F.J. Ryerson, Rutile–aqueous fluid partitioning of Nb, Ta, Hf, Zr, U, and Th: implications for high field strength element depletions in island-arc basalts, Earth Planet. Sci. Lett. 128 (1994) 327–339.
[45] J.M. Brenan, H.F. Shaw, F.J. Ryerson, D.L. Phinney, Mineral–aqueous fluid partitioning of trace elements at 900°C and 2.0 G Pa: constraints on the trace element chemistry of mantle and deep crustal fluids, Geochim. Cosmochim. Acta 59 (1995) 3331–3350.
[46] J.M. Brenan, F.J. Ryerson, H.F. Shaw, The role of aqueous fluids in the slab-to-mantle transfer of boron, beryllium

and lithium during subduction: experiments and models, Geochim. Cosmochim. Acta 62 (1998) 3337–3347.
[47] J.D. Ayers, S.K. Dittmer, G.D. Layne, Partitioning of elements between peridotite and H_2O at 2.0–3.0 GPa and 900–1000ºC, and application to models of subduction zone processes, Earth Planet. Sci. Lett. 150 (1997) 381–398.
[48] R. Stalder, S.F. Foley, G.P. Brey, I. Horn, Mineral–aqueous fluid partitioning of trace elements at 900–1200ºC and 3.0–5.7 GPa: new experimental data for garnet, clinopyroxene, and rutile, and implications for mantle metasomatism, Geochim. Cosmochim. Acta 62 (1998) 1773–1801.
[49] T. Moriguti, E. Nakamura, Across-arc variation of Li isotopes in lavas and implications for crust/mantle recycling at subduction zones, Earth Planet. Sci. Lett. 163 (1998) 167–174.
[50] G.E. Bebout, Nitrogen isotope tracers of high-temperature fluid–rock interactions: case study of the Catalina Schist, California, Earth Planet. Sci. Lett. 151 (1997) 77–90.
[51] S.S. Sorensen, J.N. Grossman, M.R. Perfit, Phengite-hosted LILE enrichment in eclogite and related rocks: implications for fluid-mediated mass transfer in subduction zones and arc magma genesis, J. Petrol. 38 (1997) 3–34.
[52] G.T. Nichols, P.J. Wyllie, C.R. Stern, Oceanic sediments: melting experiments relevant to cool subduction, in: G.E. Bebout, D.W. Scholl, S.H. Kirby, J.P. Platt (Eds.), Subduction: Top to Bottom, Am. Geophys. Union, Geophys. Monogr. 96 (1996) 293–298.
[53] G.E. Bebout, Geological and Geochemical Investigations of Fluid Flow and Mass Transfer during Subduction-Zone Metamorphism, Ph.D. Diss., Univ. Calif., Los Angeles, 1989, 370 pp.
[54] R.D. Hyndman, K. Wang, Thermal constraints on the zone of major thrust earthquake failure: the Cascadia subduction zone, J. Geophys. Res. 98 (1993) 2039–2060.
[55] W.P. Leeman, D.R. Smith, W. Hildreth, Z. Palacz, N. Rogers, Compositional diversity of late Cenozoic basalts in a transect across the southern Washington Cascades: implications for subduction zone magmatism, J. Geophys. Res. 95 (1990) 19561–19582.
[56] S.M. Peacock, Metamorphism, dehydration, and the importance of the blueschist->eclogite transition in subducting oceanic crust, Geol. Soc. Am. Bull. 105 (1993) 684–694.
[57] S.C. Ponko, S.M. Peacock, Thermal modeling of the southern Alaska subduction zone: insight into the petrology of the subducting slab and overlying mantle wedge, J. Geophys. Res. 100 (1995) 22117–22128.
[58] W.P. Leeman, Boron and other fluid-mobile elements in volcanic arc lavas: implications for subduction process, in: G.E. Bebout, D.W. Scholl, S.H. Kirby, J.P. Platt (Eds.), Subduction: Top to Bottom, Am. Geophys. Union, Geophys. Monogr. 96 (1996) 269–276.
[59] J.G. Ryan, The Systematics of Lithium, Beryllium, and Boron in Young Volcanic Rocks, Ph.D. Diss., Columbia Univ., New York, 1989, 313 pp.
[60] G.E. Bebout, E. Nakamura, T. Nakano, Boron isotope tracers of high-temperature subduction-zone fluid processes and material recycling, Abstr. Progr. Geol. Soc. Am. 30 (1998) A184.
[61] H. Becker, R.W. Carlson, K.P. Jochum, Eclogites as a monitor for trace element fractionation during devolatilization of subducted basaltic crust, Eos 77 (1997) 784.
[62] P. Philippot, P. Chevallier, C. Chopin, J. Dubessy, Fluid composition and evolution of coesite-bearing rocks (Dora-Maira massif, Western Alps): implications for element recycling during subduction, Contrib. Mineral. Petrol. 121 (1995) 29–44.
[63] Y. Tatsumi, T. Kogiso, Trace element transport during dehydration processes in the subducted oceanic crust, 2, origin of chemical and physical characteristics in arc magmatism, Earth Planet. Sci. Lett. 148 (1997) 207–221.
[64] S.S. Sorensen, Petrology of Basement Rocks of the California Continental Borderland and The Los Angeles Basin, Ph.D. Diss., Univ. Calif., Los Angeles, 1984, 423 pp.
[65] B. Altheim, Low-grade metamorphism in the Catalina Schist: kinetic and tectonic implications, M.S. Thesis, Lehigh Univ., Bethlehem, PA, 1997, 80 pp.
[66] J.G. Ryan, W.P. Leeman, J.D. Morris, C.H. Langmuir, The boron systematics of intraplate lavas: implications for crust and mantle evolution, Geochim. Cosmochim. Acta 60 (1996) 415–422.